Hindawi Publishing Corporation
EURASIP Journal on Embedded Systems
Volume 2007, Article ID 38631, 11 pages
doi:10.1155/2007/38631

Research Article

Low-Complexity Multiple Description Coding of Video Based on 3D Block Transforms

Andrey Norkin, Atanas Gotchev, Karen Egiazarian, and Jaakko Astola

Institute of Signal Processing, Tampere University of Technology, P.O. Box 553, 33101 Tampere, Finland

Received 28 July 2006; Revised 10 January 2007; Accepted 16 January 2007

Recommended by Noel Oconnor

The paper presents a multiple description (MD) video coder based on three-dimensional (3D) transforms. Two balanced descriptions are created from a video sequence. In the encoder, video sequence is represented in a form of coarse sequence approximation (shaper) included in both descriptions and residual sequence (details) which is split between two descriptions. The shaper is obtained by block-wise pruned 3D-DCT. The residual sequence is coded by 3D-DCT or hybrid, LOT+DCT, 3D-transform. The coding scheme is targeted to mobile devices. It has low computational complexity and improved robustness of transmission over unreliable networks. The coder is able to work at very low redundancies. The coding scheme is simple, yet it outperforms some MD coders based on motion-compensated prediction, especially in the low-redundancy region. The margin is up to 3 dB for reconstruction from one description.

1. INTRODUCTION

Nowadays, video is more often being encoded in mobile devices and transmitted over less reliable wireless channels. Traditionally, the objective in video coding has been to achieve high compression, which was attained with the cost of increasing encoding complexity. However, portable devices, such as camera phones, still lack enough computational power and are energy-consumption constrained. Besides, a highly compressed video sequence is more vulnerable to transmission errors, which are often present in wireless networks due to multipath fading, shadowing, and environmental noise. Thus, there is a need of a low-complexity video coder with acceptable compression efficiency and strong error-resilience capabilities.

Lower computational complexity in transform-based video coders can be achieved by properly addressing the motion estimation problem, as it is the most complex part of such coders. For the case of high and moderate frame rates ensuring smooth motion, motion-compensated (MC) prediction can be replaced by a proper transform along the temporal axis to handle the temporal correlation between frames in the video sequence. Thus, the decorrelating transform adds one more dimension, becoming a 3D one, and if a low complexity algorithm for such a transform exists, savings in overall complexity and power consumption can be expected compared to traditional video coders [1–4]. Discrete cosine transform (DCT) has been favored for its very efficient 1D implementations. As DCT is a separable transform, efficient implementations of 3D-DCT can be achieved too [2, 3, 5]. Previous research on this topic shows that simple (baseline) 3D-DCT video encoder is three to four times faster than the optimized H.263 encoder [6], for the price of some compression efficiency loss, quite acceptable for portable devices [7].

A 3D-DCT video coder is also advantageous in terms of error resilience. In MC-based coders, the decoding error would propagate further into subsequent frames until the error is corrected by an intracoded frame. The error could also spread over the bigger frame area because of motion-compensated prediction. Unlike MC-based coders, 3D-DCT video coders enjoy no error propagation in the subsequent frames. Therefore, we have chosen the 3D-DCT video coding approach for designing a low-complexity video coder with strong error resilience.

A well-known approach addressing the source-channel robustness problem is so-called multiple description coding (MDC) [8]. Multiple encoded bitstreams, called descriptions, are generated from the source information. They are correlated and have similar importance. The descriptions are independently decodable at the basic quality level and, when several descriptions are reconstructed together, improved

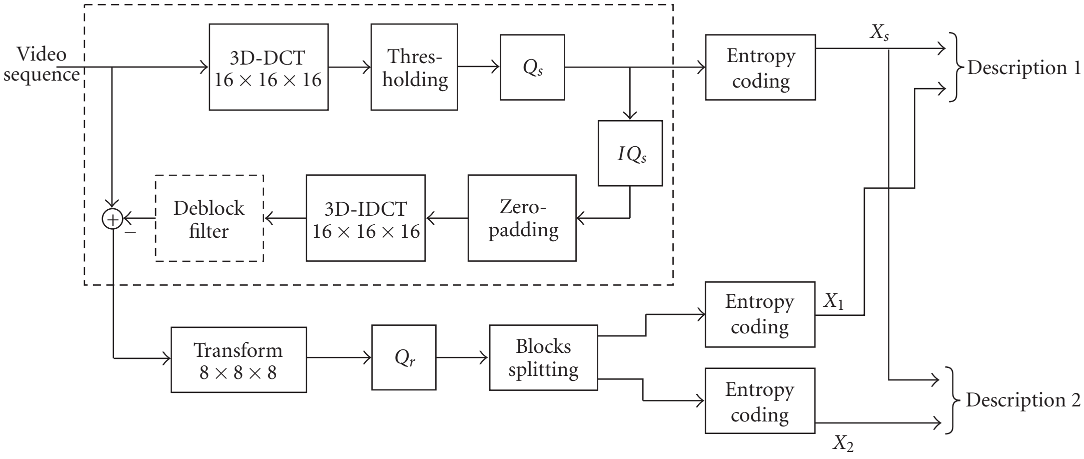

FIGURE 1: Encoder scheme.

quality is obtained. The advantages of MDC are strengthened when MDC is connected with multipath (multichannel) transport [9]. In this case, each bitstream (description) is sent to the receiver over a separate independent path (channel), which increases the probability of receiving at least one description.

Recently, a great number of multiple description (MD) video coders have appeared, most of them based on MC prediction. However, MC-based MD video coders risk having a mismatch between the prediction loops in the encoder and decoder when one description is lost. The mismatch could propagate further in the consequent frames if not corrected. In order to prevent this problem, three separate prediction loops are used at the encoder [10] to control the mismatch. Another solution is to use a separate prediction loop for every description [11, 12]. However, both approaches decrease the compression efficiency and the approach in [10] also leads to increased computational complexity and possibly to increased power consumption. A good review of MDC approaches to video coding is given in [13]. A number of MD and error-resilient video coders based on 3D transforms (e.g., wavelets, lapped orthogonal transforms (LOT), DCT) have been proposed [14–17].

In this work, we investigate a two-stage multiple description coder based on 3D transforms, denoted by *3D-2sMDC*. This coder does not exploit motion compensation as initially proposed in [18]. Using 3D transform instead of motion compensated prediction reduces the computational complexity of the coder, meanwhile eliminating the problem of mismatch between the encoder and decoder. The proposed MD video coder is a generalization of our 2-stage image MD coding approach [19] to coding of video sequences [18]. Designing the coder, we are targeting balanced computational load between the encoder and decoder. The coder should be able to work at a very low redundancy introduced by MD coding and be competitive with MD video coders based on motion-compensated prediction.

The paper is organized as follows. Section 2 overviews the encoding and decoding processes in general while Section 3 describes each block of the proposed scheme in detail. Section 4 presents the analysis of the proposed scheme and Section 5 discusses its computational complexity. Section 6 offers a packetization strategy; Section 7 presents the simulation results; while Section 8 concludes the paper.

2. GENERAL CODING SCHEME

2.1. Encoder operation

In our scheme, a video sequence is coded in two stages as shown in Figure 1. In the first stage (dashed rectangle), a coarse sequence approximation, called *shaper*, is obtained and included in both descriptions. The second stage produces enhancement information, which has higher bitrate and is split between two descriptions. The idea of the method is to get a coarse signal approximation which is the best possible for the given bitrate while decorrelating the residual sequence as much as possible.

The operation of the proposed encoder is described in the following. First, a sequence of frames is split into groups of 16 frames. Each group is split into 3D cubes of size $16 \times 16 \times 16$. 3D-DCT is applied to each cube. The lower-frequency DCT coefficients in the $8 \times 8 \times 8$ cube are coarsely quantized with quantization step Q_s and entropy-coded (see Figure 2(a)) composing the shaper, other coefficients are set to zero. Inverse quantization is applied to these coefficients followed by the inverse 3D-DCT. An optional deblocking filter serves to remove the block edges in spatial domain. Then, the sequence reconstructed from the shaper is subtracted from the original sequence to get the residual sequence.

The residual sequence is coded by a 3D block transform and transform coefficients are finely quantized with a uniform quantization step (Q_r), split into two parts in a manner shown in Figure 2(b), and entropy-coded. One part together with the shaper forms *Description 1*, while the second part combined again with the shaper forms *Description 2*. Thus, each description consists of the shaper and *half* of the transform volumes of the residual sequence.

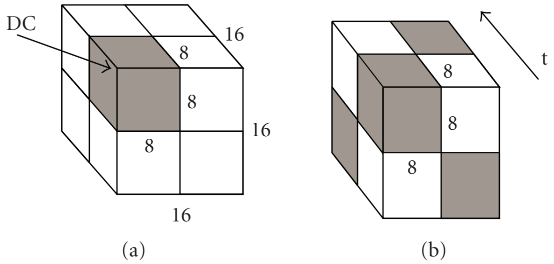

Figure 2: Coding patterns: (a) 3D-DCT cube for shaper coding: only coefficients in the gray volumes are coded, other coefficients are set to zero; (b) split pattern for volumes of a residual sequence: “gray”-*Description 1*; “white”-*Description 2*.

The shaper is included in both descriptions to facilitate successful reconstruction when one description is lost. Thus, the *redundancy* of the proposed coder is only determined by the shaper quality, which is controlled by the shaper quantization step Q_s. A larger quantization step corresponds to lower level of redundancy and lower quality of side reconstruction (reconstruction from only one description). Alternatively, a smaller quantization step results in higher-quality side reconstruction. The *quality* of the two-channel reconstruction is controlled by the quantization step Q_r used in the coding of the residual sequence. As the residual volumes are divided into two equal parts, the encoder produces balanced descriptions both in terms of PSNR and bitrate.

2.2. Decoder operation

The decoder (see Figure 3) operates as follows. When the decoder receives two descriptions, it extracts the shaper (X_s) from one of the descriptions. Then, the shaper is entropy-decoded and inverse quantization is applied. The $8 \times 8 \times 8$ volume of coefficients is zero-padded to the size $16 \times 16 \times 16$, and inverse DCT is applied. The deblocking filter is applied if it was applied in the encoder.

In case of *central* reconstruction (reconstruction from two descriptions), each part of the residual sequence (X_1 and X_2) is extracted from the corresponding description and entropy decoded. Then, volumes of the corresponding descriptions are decoded and combined together as in Figure 2(b). The inverse quantization and inverse transform (IDCT or Hybrid inverse transform) are applied to coefficients and the residual sequence is added to the shaper to obtain the reconstruction of the original sequence.

We term the reconstruction from one description, for example, *Description 1*, as *side* reconstruction (reconstruction from *Description 2* is symmetrical). The side decoder scheme can be obtained from Figure 3 if the content of the dashed rectangle is removed. In this case, the shaper is reconstructed from its available copy in *Description 1*. The residual sequence, however, has only half of the coefficient volumes (X_1). The missing volumes X_2 are simply filled with zeros. After that, the decoding process is identical to that of the central reconstruction. As the residual sequence has only half of the coefficient volumes, the side reconstruction has lower, however, still acceptable quality. For example, sequence “silent voice” coded at 64.5 kbps with 10% redundancy can be reconstructed with PSNR = 31.49 dB from two descriptions, and 26.91 dB from one description (see Table 2).

3. DETAILED SYSTEM DESCRIPTION

3.1. The coarse sequence approximation

The idea of the first coding stage is to concentrate as much information as possible into the shaper within strict bitrate constraints. We would also like to reduce artifacts and distortions appearing in the reconstructed coarse approximation. The idea is to reduce spatial and temporal resolutions of the coarse sequence approximation in order to code it more efficiently with lower bitrate [20]. Then, the original resolution sequence can be reconstructed by interpolation as a post-processing step. A good interpolation and decimation method would concentrate more information in the coarse approximation and correspondingly make the residual signal closer to white noise. A computationally inexpensive approach is to embed interpolation in the 3D transform.

The downscaling factor for the shaper was chosen equal to two in both spatial and temporal directions. The proposed scheme is able to use other downscaling factors equal to powers of two. However, the downscaling factor two has been chosen as the one producing the best results for QCIF and CIF resolutions. To reduce computational complexity, we combine downsampling with forward transform (and backward transform with interpolation). Thus, the original sequence is split into volumes of size 16 × 16 × 16, and 3D-DCT is applied to each volume. Pruned DCT is used in this stage that allows to reduce computational complexity (see Figure 2(a)). The transform size of 16 × 16 × 16 has been chosen as a compromise between the compression efficiency and computational complexity.

Only $8 \times 8 \times 8$ cubes of low-frequency coefficients in each $16 \times 16 \times 16$ coefficient volume are used; other coefficients are set to zero (see Figure 2(a)). The AC coefficients of the $8 \times 8 \times 8$ cube are uniformly quantized with quantization step Q_s. DC coefficients are quantized with the quantization step Q_{DC}.

In the $8 \times 8 \times 8$ volume, we use coefficient scanning described in [21], which is similar to a 2D zigzag scan. Although there exist more advanced types of quantization and scanning of 3D volumes [1, 22], we have found that simple scanning performs quite well. An optional deblocking filter may be used to eliminate the blocking artifacts caused by quantization and coefficient thresholding.

The DC coefficients of the transformed shaper volumes are coded by DPCM prediction. The DC coefficient of the volume is predicted from the DC coefficient of the temporally preceding volume. As the shaper is included in both descriptions, there is no mismatch between the states of the encoder and decoder when one description is lost.

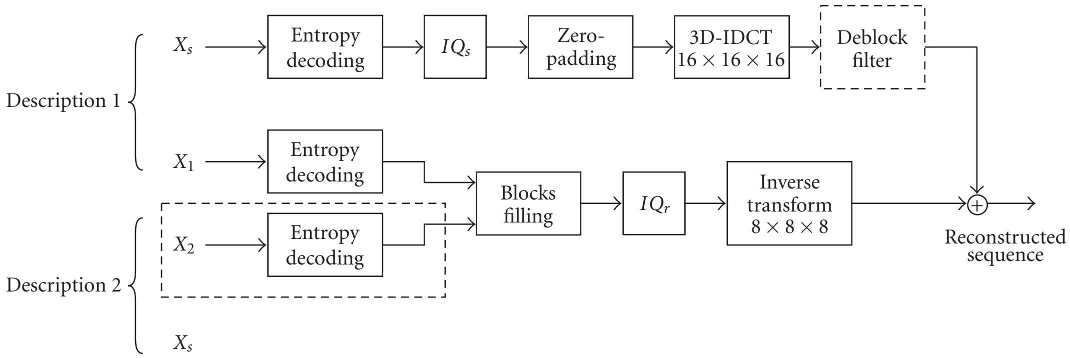

Figure 3: Decoder scheme. Central reconstruction. Side reconstruction (*Description 1*) when the content of the dashed rectangle is removed.

First, the DC coefficient prediction errors and the AC coefficients undergo zero run-length (RL) encoding. It combines runs of successive zeros and the following nonzero coefficients into two-tuples where the first number is the number of leading zeros, and the second number is the absolute value of the first nonzero coefficient following the zero-run.

Variable-length encoding is implemented as a standard Huffman encoder similar to the one in H.263 [6]. The codebook has the size 100 and is calculated for the two tuples which are the output of RL-coding. All values exceeding the range of the codebook are encoded with an "escape" code followed by the actual value. Two different codebooks are used: one for coding the shaper and another for coding the residual sequence.

3.2. Residual sequence coding

The residual sequence is obtained by subtracting the reconstructed shaper from the original sequence. As the residual sequence consists of high-frequency details, we do not add any redundancy at this stage. The residual sequence is split into groups of 8 frames in such a way that two groups of 8 frames correspond to one group of 16 frames obtained from the coarse sequence approximation. Each group of 8 frames undergoes block 3D transform. The transform coefficients are uniformly quantized with the quantization step Q_r and split between two descriptions in a pattern shown in Figure 2(b).

Two different transforms are used in this work to code the residual sequence. The first transform is 3D-DCT and the second is a hybrid transform. The latter consists of the lapped orthogonal transform (LOT) [23] in vertical and horizontal directions, and DCT in temporal direction. Both DCT and the hybrid transform produce 8 × 8 × 8 volumes of coefficients, which are split between the two descriptions. Using LOT in spatial domain smoothes blocking artifacts when reconstructing from one description. In this case, LOT spatially spreads the error caused by loosing transform coefficient blocks. Although LOT could be applied in the temporal direction to reduce blocking artifacts in temporal domain too, we avoid using it because of additional delay it introduces in the encoding and decoding processes.

As will be demonstrated in Section 7, the hybrid transform outperforms DCT in terms of PSNR and visual quality. Moreover, using LOT in spatial dimensions gives better visual results compared to DCT. However, blocking artifacts introduced by coarse coding of the shaper are not completely concealed by the residual sequence coded with the hybrid transform. These artifacts impede efficient compression of the residual sequence by the hybrid transform. Therefore, the *deblocking filter* is applied to the reconstructed shaper (see Figure 1) prior to subtracting it from the original sequence. In the experiments, we use the deblocking filter from H.263+ standard [6].

In the residual sequence coding, the transform coefficients are uniformly quantized with the quantization step Q_r. DC prediction is not used in the second stage to avoid the mismatch between the states of the encoder and decoder if one description is lost. The scanning of coefficients is 3D-zigzag scanning [21]. The entropy coding is RL coding followed by Huffman coding with a codebook different from the one used in coding the coarse sequence approximation.

4. SCHEME ANALYSIS

4.1. Redundancy and reconstruction quality

Denote by D_0 the *central distortion* (distortion when reconstructing from two descriptions), and by D_1 and D_2 the *side distortions* (distortions when reconstructing from only one description). In case of balanced descriptions, $D_1 = D_2$. Denote as D_s the distortion of the video sequence reconstructed only from the shaper. Consider 3D-DCT coding of the residual sequence. The side distortion D_1 is formed by the blocks, half of which are coded with the distortion D_0, and half with the shaper distortion D_s. Here we assume that all blocks of *Description 1* have the same expected distortion as blocks of *Description 2*. Consequently,

$$D_1 = \frac{1}{2}\left(D_s + D_0\right). \tag{1}$$

Expression (1) can also be used in case the hybrid transform is used for coding the residual. As LOT is by definition an orthogonal transform, mean-squared error distortion in spatial domain is equal to the distortion in the transform domain.

The side distortion in the transform domain is determined by loosing half of the transform coefficient blocks. Thus, expression (1) is also valid for hybrid transform. It is obvious that D_s depends on the bitrate R_s allocated to the shaper. Then, we can write (1) as

$$D_1(R_s, R_r) = \frac{1}{2}\left(D_s(R_s) + D_0(R_r, R_s)\right), \tag{2}$$

where R_r is the bitrate allocated for coding the residual sequence and R_s is the bitrate allocated to the shaper. For higher bitrates, $D_s(R_s) \gg D_0(R_r)$, and D_1 mostly depends on R_s.

The redundancy ρ of the proposed scheme is the bitrate allocated to the shaper, $\rho = R_s$. The shaper bitrate R_s and the side reconstruction distortion D_1 depend on the quantization step Q_s and the characteristics of the video sequence. The central reconstruction distortion D_0 is mostly determined by the quantization step Q_r.

Thus, the encoder has two control parameters: Q_s and Q_r. By changing Q_r, the encoder controls the central distortion. By changing Q_s, the encoder controls the redundancy and the side distortion.

4.2. *Optimization*

The proposed scheme can be optimized for changing channel behavior. Denote by p the probability of the packet loss and by R the target bitrate. Then, in case of balanced descriptions we have to minimize

$$2p(1-p)D_1 + (1-p)^2 D_0 \tag{3}$$

subject to

$$2R_s + R_r \leq R. \tag{4}$$

Taking into consideration (1), expression (3) can be transformed to the unconstrained minimization task

$$\begin{aligned} J(R_s, R_r) = {} & p(1-p)\left(D_s(R_s) + D_0(R_s, R_r)\right) \\ & + (1-p)^2 D_0(R_s, R_r) + \lambda(2R_s + R_r - R). \end{aligned} \tag{5}$$

It is not feasible to find the distortion-rate functions $D_0(R_s, R_r)$ and $D_s(R_s)$ in real-time to solve the optimization task. Instead, the distortion-rate (D-R) function of a 3D coder can be modeled as

$$D(R) = b2^{-aR} - c, \tag{6}$$

where a, b, and c are parameters, which depend on the characteristics of the video sequence. Hence,

$$D_s(R_s) = b2^{-aR_s} - c. \tag{7}$$

Assuming that the source is successively refinable in regard to the squared-error distortion measure (this is true, e.g., for i.i.d. Gaussian source [24]) we can write

$$D_0(R_s, R_r) = b2^{-a(R_s+R_r)} - c. \tag{8}$$

Then, substituting (7) and (8) into (5) and differentiating the resulting Lagrangian with respect to R_s, R_f, and λ, we can find a closed form solution of the optimization task (5). The obtained optimal values of bitrates R_s and R_r are

$$\begin{aligned} R_s^* &= \frac{1}{2}R + \frac{1}{2a}\log_2(p), \\ R_r^* &= -\frac{1}{a}\log_2(p), \end{aligned} \tag{9}$$

where R_s^* and R_r^* are rates of the shaper and the residual sequence, respectively.

Hence, the optimal redundancy ρ^* of the proposed scheme under above assumptions is

$$\rho^* = R_s^* = \frac{1}{2}R + \frac{1}{2a}\log_2(p). \tag{10}$$

The optimal redundancy ρ^* depends on the target bitrate R, the probability of packet loss p, and parameter a of the source D-R function. It does not depend on D-R parameters b and c. We have found that parameter a usually takes similar values for video sequences with the same resolution and frame rates. Thus, one does not need to estimate a in real-time. Instead, one can use a typical value of a to perform optimal bit allocation during encoding. For example, sequences with CIF resolution and 30 frames per second usually have the value of a between 34 and 44 for bitrates under 1.4 bits per pixel.

One notices that for values R and p such that $R \leq -(1/a)\log_2(p)$, the optimal redundancy ρ^* is zero or negative. For these values of R and p, the encoder should not use MDC. Instead, single description coding should be used. It is seen from (10) that the upper limit for redundancy is $R/2$, which is obtained for $p = 1$. That means that all the bits are allocated to the shaper, which is duplicated in both descriptions.

5. COMPUTATIONAL COMPLEXITY

To perform a 3D-DCT of an $N \times N \times N$ cube, one has to perform $3N^2$ one-dimensional DCTs of size N. However, if one needs only the $N/2 \times N/2 \times N/2$ low-frequency coefficients, as in the case of the shaper coding, a smaller amount of DCTs need to be computed. Three stages of separable row-column-frame (RCF) transform require $[N^2 + 1/2N^2 + 1/4N^2] = 1.75N^2$ DCTs for one cube. The same is true for the inverse transform.

The encoder needs only the 8 lowest coefficients of 1D-DCT. For this reason, we use pruned DCT as in [25]. The computation of the 8 lowest coefficients of pruned DCT II [26] of size 16 requires 24 multiplications and 61 additions [25]. That gives 2.625 multiplications and 6.672 additions per point and brings substantial reduction in computational complexity. For comparison, full separable DCT II (decimation in frequency (DIF) algorithm) [26] of size 16 would require 6 multiplications and 15.188 additions per point.

The operation count for different 3D-DCT schemes is provided in Table 1. The adopted "pruned" algorithm is compared to fast 3D vector-radix decimation-in-frequency DCT (3D VR DCT) [5] and row-column-frame (RCF) approach, where 1D-DCT is computed by DIF algorithm [26]. One can see that the adopted "pruned" algorithm has the

Table 1: Operations count for 3D-DCT II. Comparison of algorithms.

Transform	Pruned 16 × 16 × 16	3D VR 16 × 16 × 16	RCF 16 × 16 × 16	3D VR 8 × 8 × 8	RCF 8 × 8 × 8
Mults/point	2.625	3.5	6	2.625	4.5
Adds/point	6.672	15.188	15.188	10.875	10.875
Mults+adds/point	9.297	18.688	21.188	13.5	15.375

lowest computational complexity. In terms of operations per pixel, partial DCT 16 × 16 × 16 is less computationally expensive than full 8 × 8 × 8 DCT used to code the residual sequence.

In [7], a baseline 3D-DCT encoder is compared to the optimized H.263 encoder [27]. It was found [7] that baseline 3D-DCT encoder is up to four times faster than the optimized H.263 encoder. In the baseline 3D-DCT encoder [7], DCT was implemented by RCF approach, which gives 15.375 operations/point. In our scheme, forward pruned 3D-DCT for the shaper requires only 9.3 op/point. Adding the inverse transform, one gets 18.6 op/points. The 8 × 8 × 8 DCT of the residual sequence can be implemented by 3D VR DCT [5], which requires 13.5 op/point. Thus, the overall complexity of the transforms used in the proposed encoder is estimated as 32.1 op/point, that is about twice higher than the complexity of the transforms used in baseline 3D-DCT (15.375 op/point).

The overall computational complexity of the encoder includes quantization and entropy coding of the shaper coefficients. However, the number of coefficients coded in the shaper is eight times lower than the number of coefficients in the residual sequence as only 512 lower DCT coefficients in each 16×16×16 block are coded. Thus, quantization and entropy coding of the shaper would take about 8 times less computations than quantization and entropy coding of the residual sequence. Thus, we estimate that the overall complexity of the proposed encoder is not more than twice the complexity of baseline 3D-DCT [7]. This means that the proposed coder has up to two times lower-computational complexity than the optimized H.263 [27]. The difference in computational complexity between the proposed coder and H.263+ with scalability (providing error resilience) is even bigger. However, the proposed coder has single description performance similar or even higher than H.263+ [6] with SNR scalability, as shown in Section 7.

6. PACKETIZATION AND TRANSMISSION

The bitstream of the proposed video coder is packetized as follows. A group of pictures (16 frames) is split into 3D-volumes of size 16 × 16 × 16. One packet should contain one or more shaper volumes, which gives 512 entropy-coded coefficients (due to thresholding).

In case of single description coding, one shaper volume is followed by eight spatially corresponding volumes of the residual sequence, which have the size of 8 × 8 × 8. In case of multiple description coding, a packet from *Description 1* contains a shaper volume and four residual volumes taken in the pattern shown in Figure 2(b). *Description 2* contains the same shaper volume and four residual volumes, which are not included into *Description 1*. If the size of such a block (one shaper volume and four residual volumes) is small, several blocks are packed into one packet.

The proposed coder uses DPCM prediction of DC coefficients in the shaper volumes. The DC coefficient is predicted from the DC coefficient of the temporally preceding volume. If both descriptions containing the same shaper volume are lost, DC coefficient is estimated as the previous DC coefficient in the same spatial location or as an average of DC coefficients of the spatially adjacent volumes. This concealment may introduce mismatch in DPCM loop between the encoder and decoder. However, the mismatch does not spread out of the border of this block. The mismatch is corrected by the DC coefficient update which can be requested over a feedback channel or may be done periodically.

To further improve the robustness against burst errors, the bitstream can be reordered in a way that descriptions corresponding to one 3D volume are transmitted in the packets which are not consecutive. It will decrease the probability that both descriptions are lost due to consequent packet losses. Another solution to improve the error resilience is to send the packets of *Description 1* over one link, and packets from *Description 2* over another link.

7. SIMULATION RESULTS

This section presents the comparison of the proposed MD coder with other MD coders. The experiments are performed on sequences "Tempete" (CIF, 30 fps, 10 s), "silent voice" (QCIF, 15 fps, 10 s), and "Coastguard" (CIF, 30 fps). We measure the reconstruction quality by using the *peak signal-to-noise ratio* (PSNR). The distortion is average luminance PSNR over time, all color components are coded. We compare our scheme mainly with H.263-based coders as our goal is low-complexity encoding. Apparently, the proposed scheme cannot compete with H.264 in terms of compression performance. However, H.264 encoders are much more complex.

7.1. Single description performance

Figure 4 plots PSNR versus bitrate for the sequence "Tempete." The compared coders are single description coders. "3D-2stage" coder is a single-description variety of the coder described above. The shaper is sent only once, and the residual sequence is sent in a single description. "3D-DCT" is a simple 3D-DCT coder described in [1, 7]. "H.263" is a Telenor implementation of H.263. "H.263-SNR" is an H.263+ with SNR scalability, implemented at the University

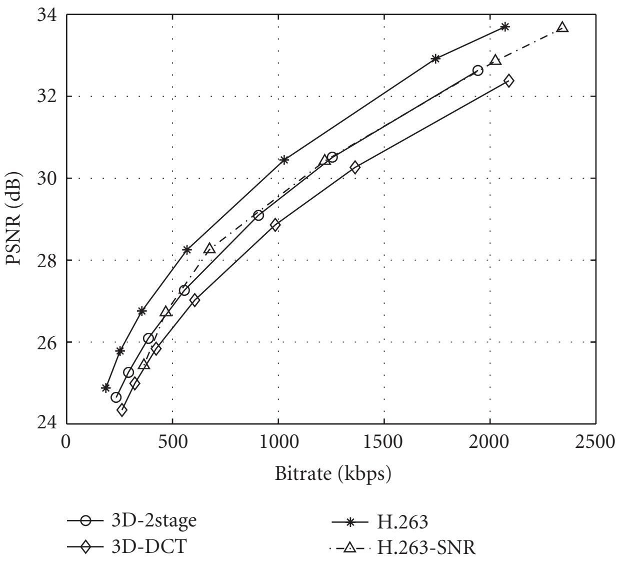

FIGURE 4: Sequence "Tempete," single description coding.

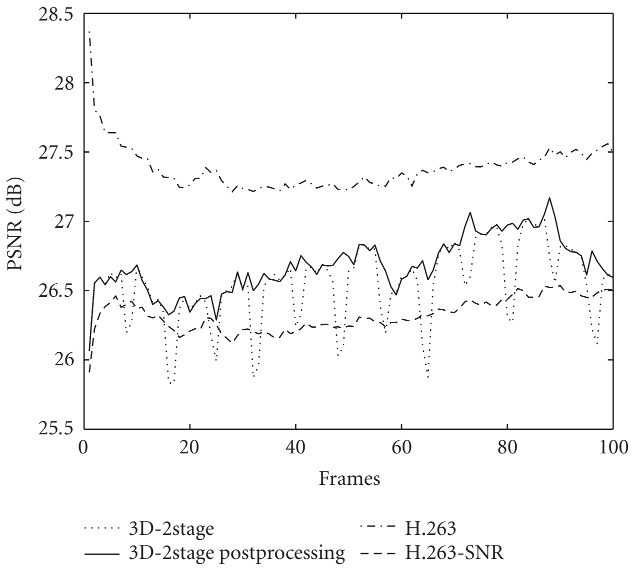

FIGURE 5: Sequence "Tempete" coded at 450 kbps, single description coding.

of British Columbia [28, 29]. One can see that H.263 coder outperforms other coders. Our 3D-2stage has approximately the same performance as H.263+ with SNR scalability and its PSNR is half to one dB lower than that of H.263+. Simple 3D-DCT coder showed the worst performance.

Figure 5 shows PSNR of the first 100 frames of "Tempete" sequence. The sequence is encoded to target bitrate 450 kbps. Figure 5 demonstrates that 3D-DCT coding exhibits temporal degradation of quality on the borders of 8-frame blocks. These temporal artifacts are caused by block-wise DCT and perceived like abrupt movements. These artifacts can be efficiently concealed with postprocessing on the decoder side. In this experiment, we applied MPEG-4 deblocking filter [30] to block borders in temporal domain. As a result, temporal artifacts are smoothed. The perceived quality of the video sequence has also improved. Some specialized methods for deblocking in temporal domain can be applied as in [31]. Postprocessing in temporal and spatial domains can also improve reconstruction quality in case of description loss. In the following experiments, we do not use postprocessing in order to have fair comparison with other MDC methods.

7.2. Performance of different residual coding methods

In the following, we compare the performance of MD coders in terms of side reconstruction distortion, while they have the same central distortion. Three variants of the proposed 3D-2sMDC coder are compared. These MD coders use different schemes for coding the residual sequence. "Scheme 1" is the 2-stage coder, which uses hybrid transform for the residual sequence coding and the deblocking filtering of the shaper. "Scheme 2" employs DCT for coding the residual sequence. "Scheme 3" is similar to "Scheme 2" except that it uses the deblocking filter (see Figure 1). We have compared these schemes with simple MD coder based on 3D-DCT and MDSQ [32]. MDSQ is applied to the first N coefficients of $8 \times 8 \times 8$ 3D-DCT cubes. Then, MDSQ indices are sent to corresponding descriptions, and the rest of $512 - N$ coefficients are split between two descriptions (even coefficients go to Description 1 and odd coefficients to Description 2).

Figure 6 shows the result of side reconstruction for the reference sequence "Tempete." The average central distortion (reconstruction from both descriptions) is fixed for all encoders, $D_0 = 28.3$ dB. The mean side distortion (reconstruction from one description) versus bitrate is compared. One can see that "Scheme 1" outperforms other coders, especially in the low-redundancy region. One can also see that the deblocking filtering applied to the shaper ("Scheme 3") does not give much advantage for the coder using 3D-DCT for coding the residual sequence. However, the deblocking filtering of the shaper is necessary in "Scheme 1" as it considerably enhances visual quality. The deblocking filtering requires twice less operations comparing to the sequence of the same format in H.263+ because the block size in the shaper is twice larger than that in H.263+. All the three variants of our coder outperform the "3D-MDSQ" coder to the extent of 2 dB.

7.3. Network performance of the proposed method

Figure 7 shows performance of the proposed coder in network environment with error bursts. In this experiment, bursty packet loss behavior is simulated by a two-state Markov model. These two states are G (good) when packets are correctly received and B (bad) when packets are either lost or delayed. This model is fully described by transition probabilities p_{BG} from state B to state G and p_{GB} from G to B.

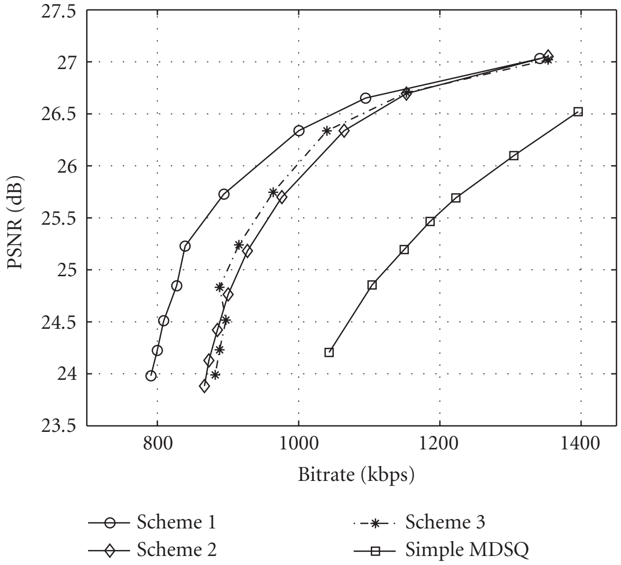

Figure 6: Sequence “Tempete,” 3D-2sMDC, mean side reconstruction. $D_0 \approx 28.3$ dB.

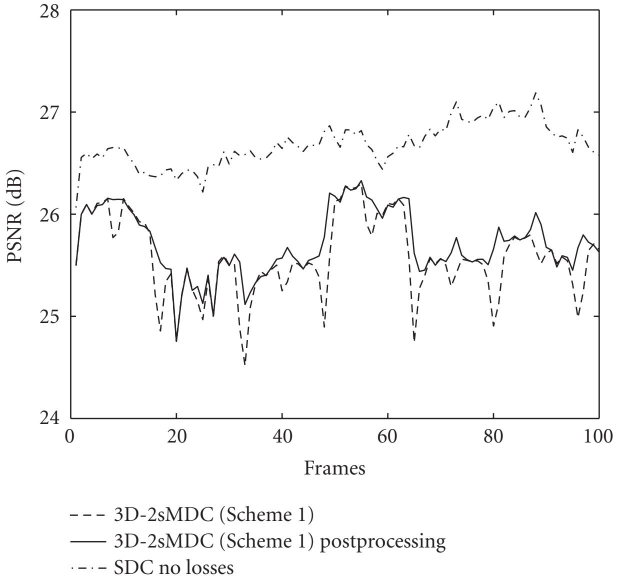

Figure 7: Network performance, packet loss rate 10%. Sequence “Tempete,” coded at 450 kbps. Comparison of 3D-2sMDC and 3D-2sMDC with posfiltering. Performance of single description coder without losses is given as a reference.

The model can also be described by average loss probability $P_B = \Pr(B) = p_{GB}/(p_{GB} + p_{BG})$ and the average burst length $L_B = 1/p_{BG}$.

In the following experiment, the sequence “Tempete” (CIF, 30 fps) has been coded to bitrate 450 kbps into packets not exceeding the size of 1000 bytes for one packet. The coded sequence is transmitted over two channels modeled by two-state Markov models with $P_B = 0.1$ and $L_B = 5$. Packet losses in *Channel 1* are uncorrelated with errors in *Channel 2*. Packets corresponding to *Description 1* are transmitted over *Channel 1*, and packets corresponding to *Description 2* are transmitted over *Channel 2*. Two channels are used to unsure uncorrelated losses of Description 1 and Description 2. Similar results can be achieved by interleaving packets (descriptions) corresponding to the same spatial locations. When both descriptions are lost, error concealment described in Section 6 is used. Optimal redundancy for “Tempete” sequence estimated by (10) for bitrate 450 kbps (0.148 bpp) is 21%.

Figure 7 shows network performance of 3D-2sMDC and 3D-2sMDC with postrocessing (temporal deblocking). The performance of a single description 3D-2stage coder with postprocessing in a lossless environment is also given in Figure 7 as a reference. One can see that using MDC for error resilience helps to maintain an acceptable level of quality when transmitting over network with packet losses.

7.4. Comparison with other MD coders

The next set of experiments is performed on the first 16 frames of the reference sequence “Coastguard” (CIF, 30 fps). The first coder is the proposed 3D-2sMDC coder Scheme 1. The “H.263 spatial” method exploits H.263+ [29] to generate layered bitstream. The base layer is included in both descriptions while the enhancement layer is split between two descriptions on a GOB basis. The “H.263 SNR” is similar to the previous method with the difference that it uses SNR scalability to create two layers.

Figure 8 plots the single description distortion versus bitrate of the “Coastguard” sequence for the three coders described above. The average central distortion is $D_0 = 28.5$ dB. One can see that 3D-2stage method outperforms the two other methods.

The results indicate that the proposed MD coder based on 3D transforms outperforms simple MD coders based on H.263+ and the coder based on MDSQ and 3D-DCT. For the coder with SNR scalability, we were not able to get the bitrates as low as we have got with our “3D-2stage” method.

Another set of experiments is performed on the reference sequence “Silent voice” (QCIF, 15 fps). The proposed 3D-2sMDC coder is compared with MDTC coder that uses three prediction loops in the encoder [10, 33]. The 3D-2sMDC coder exploits “Scheme 1” as in the previous set of experiments. The rate-distortion performance of these two coders is shown in Figure 9. The PSNR of two-description reconstruction of 3D-2sMDC coder is $D_0 = 31.47 - 31.57$ dB and central distortion of MDTC coder is $D_0 = 31.49$ dB.

The results show that the proposed 3D-2sMDC coder outperforms the MDTC coder, especially in a low-redundancy region. The superior side reconstruction performance of our coder could be explained by the following. MC-based multiple description video coder has to control the mismatch between the encoder and decoder. It could be done, for example, by explicitly coding the mismatch signal, as it is done in [10, 33]. In opposite, MD coder based on 3D transforms does not need to code the residual signal, thus,

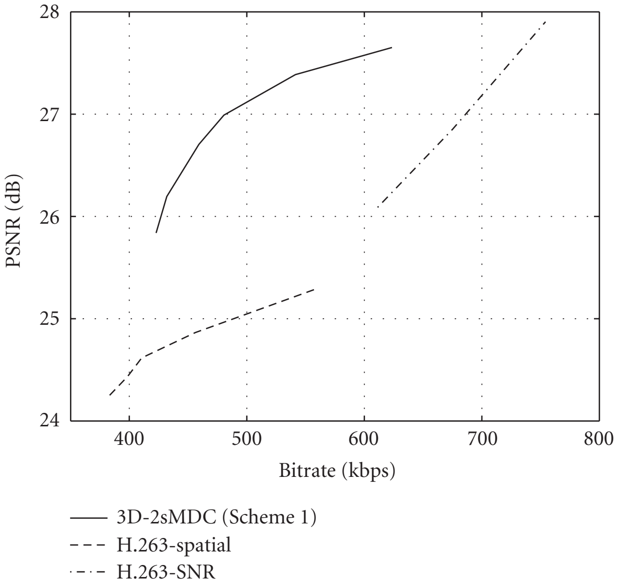

FIGURE 8: Sequence "Coastguard," mean side reconstruction. $D_0 \approx$ 28.5 dB.

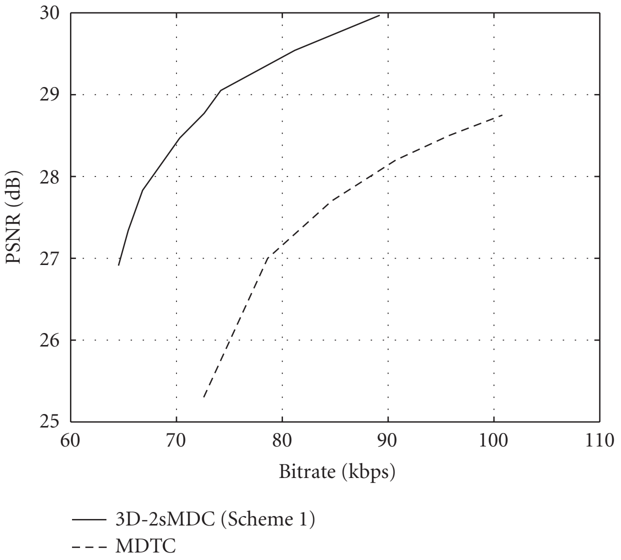

FIGURE 9: Sequence "Silent voice," mean side reconstruction. $D_0 \approx$ 31.53 dB.

TABLE 2: Reconstruction results. Sequence "Silent voice."

Central PSNR (dB)	Mean side PSNR (dB)	Bitrate (kbps)	Redundancy (%)
31.49	26.91	64.5	9.8
31.51	27.34	65.5	11.4
31.51	27.83	66.8	13.7
31.57	28.47	70.3	19.6
31.52	29.05	74.2	26.3
31.47	29.54	81.2	38.2
31.53	29.97	89.2	51.8

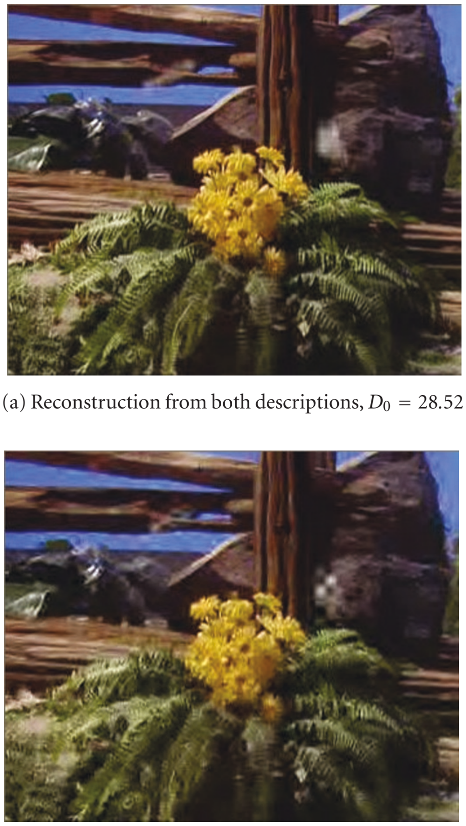

(a) Reconstruction from both descriptions, $D_0 = 28.52$

(b) Reconstruction from *Description 1*, $D_1 = 24.73$

FIGURE 10: Sequence "Tempete," frame 13.

gaining advantage of very low redundancies (see Table 2). The redundancy in Table 2 is calculated as the additional bitrate for MD coder comparing to the single description 2-stage coder based on 3D transforms.

A drawback of our coder is relatively high delay. High delays are common for coders exploiting 3D transforms (e.g., coders based on 3D-DCT or 3D-wavelets). Waiting for 16 frames to apply 3D transform introduces additional delay of slightly more than half a second for the frame rate 30 fps and about one second for 15 fps. The proposed coder also needs larger memory than MC-based video coder, as it is required to keep the 16 frames in the buffer before applying the DCT. This property is common for most of 3D transform video coders. We suppose that most of modern mobile devices have enough memory to perform the encoding.

Figure 10 shows frame 13 of the reference sequence Tempete reconstructed from both descriptions (Figure 10(a)) and from *Description 1* alone (Figure 10(b)). The sequence is coded by 3D-2sMDC (Scheme 1) encoder to bitrate R = 880 kbps. One can see that although the image reconstructed from one description has some distortions caused by loss of transform coefficient volumes of the residual sequence, the overall picture is smooth and pleasant to the eye.

8. CONCLUSION

We have proposed an MDC scheme for coding of video which does not use motion-compensated prediction. The coder exploits 3D transforms to remove correlation in video sequence. The coding process is done in two stages: the first stage produces coarse sequence approximation (shaper) trying to fit as much information as possible in the limited bit budget. The second stage encodes the residual sequence, which is the difference between the original sequence and the shaper-reconstructed one. The shaper is obtained by pruned 3D-DCT, and the residual signal is coded by 3D-DCT or hybrid 3D transform. The redundancy is introduced by including the shaper in both descriptions. The amount of redundancy is easily controlled by the shaper quantization step. The scheme can also be easily optimized for suboptimal bit allocation. This optimization can run in real time during the encoding process.

The proposed MD video coder has low computational complexity, which makes it suitable for mobile devices with low computational power and limited battery life. The coder has been shown to outperform MDTC video coder and some simple MD coders based on H.263+. The coder performs especially well in a low-redundancy region. The encoder is also less computationally expensive than the H.263 encoder.

ACKNOWLEDGMENT

This work is supported by the Academy of Finland, Project no. 213462 (Finnish Centre of Excellence program (2006–2011)).

REFERENCES

[1] R. K. Chan and M. C. Lee, "3D-DCT quantization as a compression technique for video sequences," in *Proceedings of the Annual International Conference on Virtual Systems and Multimedia (VSMM '97)*, pp. 188–196, Geneva, Switzerland, September 1997.

[2] S. Saponara, L. Fanucci, and P. Terreni, "Low-power VLSI architectures for 3D discrete cosine transform (DCT)," in *Proceedings of the 46th IEEE International Midwest Symposium on Circuits and Systems (MWSCAS '03)*, vol. 3, pp. 1567–1570, Cairo, Egypt, December 2003.

[3] A. Burg, R. Keller, J. Wassner, N. Felber, and W. Fichtner, "A 3D-DCT real-time video compression system for low complexity single-chip VLSI implementation," in *Proceedings of the Mobile Multimedia Conference (MoMuC '00)*, p. 1B-5-1, Tokyo, Japan, November 2000.

[4] M. Bakr and A. E. Salama, "Implementation of 3D-DCT based video encoder/decoder system," in *Proceedings of the 45th IEEE Midwest Symposium on Circuits and Systems (MWSCAS '02)*, vol. 2, pp. 13–16, Tulsa, Okla, USA, August 2002.

[5] S. Boussakta and H. O. Alshibami, "Fast algorithm for the 3-D DCT-II," *IEEE Transactions on Signal Processing*, vol. 52, no. 4, pp. 992–1001, 2004.

[6] ITU-T, *Video coding for low bitrate communication*. ITU-T Recommendation, Draft on H.263v2, 1999.

[7] J. J. Koivusaari and J. H. Takala, "Simplified three-dimensional discrete cosine transform based video codec," in *Multimedia on Mobile Devices*, vol. 5684 of *Proceedings of SPIE*, pp. 11–21, San Jose, Calif, USA, January 2005.

[8] V. K. Goyal, "Multiple description coding: compression meets the network," *IEEE Signal Processing Magazine*, vol. 18, no. 5, pp. 74–93, 2001.

[9] J. G. Apostolopoulos and S. J. Wee, "Unbalanced multiple description video communication using path diversity," in *Proceedings of IEEE International Conference on Image Processing (ICIP '01)*, vol. 1, pp. 966–969, Thessaloniki, Greece, October 2001.

[10] A. R. Reibman, H. Jafarkhani, Y. Wang, M. T. Orchard, and R. Puri, "Multiple description coding for video using motion compensated prediction," in *Proceedings of IEEE International Conference on Image Processing (ICIP '99)*, vol. 3, pp. 837–841, Kobe, Japan, October 1999.

[11] J. G. Apostolopoulos, "Error-resilient video compression through the use of multiple states," in *Proceedings of IEEE International Conference on Image Processing (ICIP '00)*, vol. 3, pp. 352–355, Vancouver, BC, Canada, September 2000.

[12] V. Vaishampayan and S. A. John, "Balanced interframe multiple description video compression," in *Proceedings of IEEE International Conference on Image Processing (ICIP '99)*, vol. 3, pp. 812–816, Kobe, Japan, October 1999.

[13] Y. Wang, A. R. Reibman, and S. Lin, "Multiple description coding for video delivery," *Proceedings of the IEEE*, vol. 93, no. 1, pp. 57–70, 2005.

[14] H. Man, R. L. de Queiroz, and M. J. T. Smith, "Three-dimensional subband coding techniques for wireless video communications," *IEEE Transactions on Circuits and Systems for Video Technology*, vol. 12, no. 6, pp. 386–397, 2002.

[15] J. Kim, R. M. Mersereau, and Y. Altunbasak, "Error-resilient image and video transmission over the Internet using unequal error protection," *IEEE Transactions on Image Processing*, vol. 12, no. 2, pp. 121–131, 2003.

[16] S. Somasundaram and K. P. Subbalakshmi, "3-D multiple description video coding for packet switched networks," in *Proceedings of IEEE International Conference on Multimedia and Expo (ICME '03)*, vol. 1, pp. 589–592, Baltimore, Md, USA, July 2003.

[17] M. Yu, Z. Wenqin, G. Jiang, and Z. Yin, "An approach to 3D scalable multiple description video coding with content delivery networks," in *Proceedings of IEEE International Workshop on VLSI Design and Video Technology (IWVDVT '05)*, pp. 191–194, Suzhou, China, May 2005.

[18] A. Norkin, A. Gotchev, K. Egiazarian, and J. Astola, "A low-complexity multiple description video coder based on 3D-transforms," in *Proceedings of the 14th European Signal Processing Conference (EUSIPCO '06)*, Florence, Italy, September 2006.

[19] A. Norkin, A. Gotchev, K. Egiazarian, and J. Astola, "Two-stage multiple description image coders: analysis and comparative study," *Signal Processing: Image Communication*, vol. 21, no. 8, pp. 609–625, 2006.

[20] A. M. Bruckstein, M. Elad, and R. Kimmel, "Down-scaling for better transform compression," *IEEE Transactions on Image Processing*, vol. 12, no. 9, pp. 1132–1144, 2003.

[21] B.-L. Yeo and B. Liu, "Volume rendering of DCT-based compressed 3D scalar data," *IEEE Transactions on Visualization and Computer Graphics*, vol. 1, no. 1, pp. 29–43, 1995.

[22] N. Bozinovic and J. Konrad, "Motion analysis in 3D DCT domain and its application to video coding," *Signal Processing: Image Communication*, vol. 20, no. 6, pp. 510–528, 2005.

[23] H. S. Malvar and D. H. Staelin, "The LOT: transform coding without blocking effects," *IEEE Transactions on Acoustics, Speech, and Signal Processing*, vol. 37, no. 4, pp. 553–559, 1989.

[24] W. H. R. Equitz and T. M. Cover, "Successive refinement of information," *IEEE Transactions on Information Theory*, vol. 37, no. 2, pp. 269–275, 1991.

[25] A. N. Skodras, "Fast discrete cosine transform pruning," *IEEE Transactions on Signal Processing*, vol. 42, no. 7, pp. 1833–1837, 1994.

[26] K. Rao and R. Yip, *Discrete Cosine Transform: Algorithms, Advantages, Applications*, Academic Press, London, UK, 1990.

[27] K. Yu, J. Lv, J. Li, and S. Li, "Practical real-time video codec for mobile devices," in *Proceedings of IEEE International Conference on Multimedia and Expo (ICME '03)*, vol. 3, pp. 509–512, Baltimore, Md, USA, July 2003.

[28] G. Cote, B. Erol, M. Gallant, and F. Kossentini, "H.263+: video coding at low bitrates," *IEEE Transactions on Circuits and Systems for Video Technology*, vol. 8, no. 7, pp. 849–866, 1998.

[29] L. Roberts, "TMN 8 (h.263+) encoder/decoder, version 3.0," 1997, Signal Processing and Multimedia Laboratory, Univiversity of British Columbia, Vancouver, BC, Canada, May, 1997.

[30] S. D. Kim, J. Yi, H. M. Kim, and J. B. Ra, "A deblocking filter with two separate modes in block-based video coding," *IEEE Transactions on Circuits and Systems for Video Technology*, vol. 9, no. 1, pp. 156–160, 1999.

[31] D. Rusanovskyy and K. Egiazarian, "Post-processing for three-dimensional discrete cosine transform based video coding," in *Proceedings of the 7th International Conference on Advanced Concepts for Intelligent Vision Systems (ACIVS '05)*, pp. 618–625, Antwerp, Belgium, September 2005.

[32] V. Vaishampayan, "Design of multiple description scalar quantizers," *IEEE Transactions on Information Theory*, vol. 39, no. 3, pp. 821–834, 1993.

[33] A. R. Reibman, H. Jafarkhani, Y. Wang, M. T. Orchard, and R. Puri, "Multiple-description video coding using motion-compensated temporal prediction," *IEEE Transactions on Circuits and Systems for Video Technology*, vol. 12, no. 3, pp. 193–204, 2002.